Am J Cancer Res 2016;6(4):764-780
www.ajcr.us /ISSN:2156-6976/ajcr0024919

Original Article

Chronic oxidative stress increases the integration frequency of foreign DNA and human papillomavirus 16 in human keratinocytes

Yan Chen Wongworawat, Maria Filippova, Vonetta M Williams, Valery Filippov, Penelope J Duerksen-Hughes

Department of Basic Science, Loma Linda University School of Medicine, Loma Linda, CA, USA

Received January 25, 2016; Accepted February 3, 2016; Epub March 15, 2016; Published April 1, 2016

Abstract: Cervical cancer is the second most common cancer, and the fourth most common cause of cancer death in women worldwide. Nearly all of these cases are caused by high-risk HPVs (HR HPVs), of which HPV16 is the most prevalent type. In most cervical cancer specimens, HR HPVs are found integrated into the human genome, indicating that integration is a key event in cervical tumor development. An understanding of the mechanisms that promote integration may therefore represent a unique opportunity to intercept carcinogenesis. To begin identifying these mechanisms, we tested the hypothesis that chronic oxidative stress (OS) induced by virus- and environmentally-mediated factors can induce DNA damage, and thereby increase the frequency with which HPV integrates into the host genome. We found that virus-mediated factors are likely involved, as expression of E6*, a splice isoform of HPV16 E6, increased the levels of reactive oxygen species (ROS), caused oxidative DNA damage, and increased the frequency of plasmid DNA integration as assessed by colony formation assays. To assess the influence of environmentally induced chronic OS, we used L-Buthionine-sulfoximine (BSO) to lower the level of the intracellular antioxidant glutathione. Similar to our observations with E6*, glutathione depletion by BSO also increased ROS levels, caused oxidative DNA damage and increased the integration frequency of plasmid DNA. Finally, under conditions of chronic OS, we were able to induce and characterize a few independent events in which episomal HPV16 integrated into the host genome of cervical keratinocytes. Our results support a chain of events leading from induction of oxidative stress, to DNA damage, to viral integration, and ultimately to carcinogenesis.

Keywords: Cervical cancer, high-risk HPVs (HR HPVs), integration, oxidative stress (OS), reactive oxygen species (ROS), E6*, carcinogenesis

Introduction

Cervical cancer is the second most common cancer in women, and the fourth most common cause of cancer-related death in women worldwide [1, 2]. Human papilloma virus (HPV) infection is well-established as the causative agent of cervical cancer [3], and at least 85% of pre-malignant and 90% of malignant squamous lesions in the uterine cervix test HPV DNA positive [4]. High-risk HPV such as HPV type 16 is the most prevalent type and accounts for more than 50% of all cases of cervical cancer [5].

Over-expression of the HR E6 and E7 oncoproteins are considered responsible for most malignancies. This over-expression can be triggered by several mechanisms, including epigenetic modifications of the HPV genome [6]. However, integration of the HPV genome into that of the host, with an accompanying loss of E2 and the resulting over-expression of E6 and E7, appears to be one of the most common oncogenic pathways [7]. Following viral infection, the HPV genome is present in episomal form, with low levels of E6 and E7 oncoprotein expression due to the suppressive activity of E2 [8]. The level of oncogene expression grows with increase of virus load [9] and following integrative events that disable E2-mediated suppression of E6 and E7 [8]. Clinical data support this sequence, as precancerous lesions CIN1 and CIN2 display episomal viral genomes [10], while rapid progression of CIN lesions is closely associated with integrated HPV16 [11] and is accompanied by increased levels of E6 and E7 expression. In 88% of specimens obtained from cervical cancers, HPV DNA is found integrated into host genomes [12].

Integration requires linearization of the viral genome and breakage of the host genome, along with the ability to re-ligate the ends together. Therefore, agents that cause DNA breakage are predicted to increase integration frequency. Perhaps the most common agents of DNA damage are reactive oxygen radicals (ROS). Indeed, in the case of hepatitis B virus (HBV), oxidative stress (OS) has been shown to enhance viral integration by increasing DNA damage [13, 14]; this integration then serves as a key step during HBV-initiated carcinogenesis [15]. OS can be generated both by the virus itself and through environmental agents. Virus infection alone has the potential to induce OS, as seen in cases such as HBV and Epstein-Barr virus (EBV) [16-19]. In contrast to the situation seen with these two viruses, infection with HPV does not in itself seem to cause significant inflammation likely to lead to OS, suggesting that any connection between HPV and OS is likely mediated by specific proteins. Support for a connection between specific HPV proteins and integration, possibly mediated by increased OS, is provided by the observation that expression of HR HPV E6 and E7 can promote integration of a reporter plasmid [20]. Previous work from our laboratory demonstrated that at least one HPV-encoded protein, E6*, is able to increase ROS levels and DNA damage [21]. E6* is a splice variant of E6; interestingly, the full-length E6 protein does not affect ROS levels in the host cell [21]. We also showed that an E6*-mediated increase in ROS is connected to a decrease in the expression of antioxidant enzymes such as superoxide dismutase (SOD2) and glutathione peroxidase (GPx ½) [21].

In addition to such viral contributions to OS, environmental contributions are also likely. For example, epidemiological data link conditions known to cause oxidative stress and DNA damage, such as smoking and co-infection with the STD-associated pathogens *Chlamydia trachomatis* and *Neisseria gonorrhoeae*, with increased incidence of HPV-mediated cancers [22-28], while corroborating data from the Ozbun lab demonstrated that tobacco exposure increased E6/E7 oncogene expression, DNA damage and mutation rates in cells carrying HPV episomes [29], and that nitric oxide increases DNA damage in HPV positive cells [30].

However, the mechanistic link between OS and HPV DNA integration has not yet been examined, leading us to ask if we could induce HPV integration by generating OS-induced DNA damage. To investigate the relationship between chronic OS, DNA damage, and the rate at which episomal HPV DNA integrates into the cellular genome, we first performed a validation study using a U2OS cell line model and found that overexpression of E6* increased the rate of circular plasmid DNA integration, while manipulating the level of OS modified the integration frequency. We were also able to demonstrate the relationship between OS induction, DNA damage and increased plasmid integration in Normal Oral Keratinocytes (NOK cells). Finally, by treating Human Cervical Keratinocytes (HCK, which normally carry the HPV episome) with the glutathionine-depleting agent L-Buthionine-sulfoximine (BSO), we were able to increase the rate at which the HPV episome integrated into the genomic DNA. In summary, we found that chronic OS, caused either by E6* overexpression or by BSO treatment, increased the levels of cellular DNA damage, leading to an increased frequency of integration for plasmid and episomal HPV16 DNA.

Materials and methods

Reagents

L-Buthionine-sulfoximine (BSO) was purchased from Sigma-Aldrich (St. Louis, MO). Stock solution, at a concentration of 100 mM, was prepared in phosphate-buffered saline (PBS) and kept at -20°C. Vitamin E and Resveratrol were purchased from Sigma-Aldrich (St. Louis, MO). Flag-agarose and anti-Flag-HRP antibodies were purchased from Sigma-Aldrich (St. Louis, MO).

Cell culture

U2OS cells derived from a human osteosarcoma were obtained from the ATCC (Manassas, VA), and were cultured in McCoy's 5A medium (Invitrogen, Carlsbad, CA) that was supplemented to contain 10% fetal bovine serum (FBS) (Invitrogen). The U2OS cell line was authenticated by ATCC short tandem repeat profiling in November, 2015 and exhibited no evidence of cross-contamination with known ATCC cell lines.

Normal oral keratinocytes (NOKs), non-transformed cells immortalized by Human Telomerase Reverse Transcriptase (hTERT) that were kindly provided by Dr. Karl Münger [31], were

grown in keratinocyte serum-free medium (Invitrogen, Carlsbad, CA).

Human cervical keratinocytes (HCK) containing episomal HPV16, kindly provided by Dr. Aloysius J. Klingelhutz [32], were grown in E-media [33].

All media were supplemented with penicillin (100 U/ml) and streptomycin (100 µg/ml) (Sigma-Aldrich, St. Louis, MO).

Transfections and transductions

Transfections were performed following the protocol provided with the TransIT-2020 reagent kit (Mirus Bio, Madison, WI). Briefly, U2OS or NOK cells were transfected with plasmids encoding E6* (pE6*), E6 large (pE6 large) or the empty vector (pFlag). To normalize for transfection efficiency, pMetLuc was co-transfected, following the protocol provided with the TransIT-keratinocyte transfection reagent kit (Mirus Bio, Madison, WI). Expression of MetLuc was monitored in the media, and these values used for normalization.

Stable clones were obtained by transduction of retroviruses pLNCX, pLNCX-E6*, or pLNCX-E6 into NOK cells. Individual selected clones were analysed for protein expression by immunoblotting and/or real-time PCR as described previously [21].

Clonogenic assay

5×10^5 cells were transfected with pMetluc and incubated for 48 hours under cell culture conditions, followed by the addition of appropriate antibiotics (*G418* at a concentration of 0.5 mg/ml for U2OS cells or *puromycin* at a concentration of 5 µg/ml for NOK cells) and selection for 2-3 weeks. After antibiotic selection, colonies were fixed using 10% formaldehyde for 30-45 min. After rinsing with water and drying overnight at room temperature, cells were stained with 1% crystal violet for 45-60 min. Dishes were rinsed with water and left to dry overnight at room temperature. Colonies were counted the following day.

Immunoprecipitation

10^6 cells from each assessed U2OS preparation, transiently transfected with plasmids encoding E6* (pE6*), E6 large (pE6L) or vector (pFlag), were lysed using lysis buffer [34]. Flag-tagged proteins were then precipitated using Flag-agarose, and bound proteins were subjected to SDS-PAGE. Following transfer to a polyvinylidene difluoride (PVDF) membrane, the Flag-E6* and Flag-E6 proteins were detected by immunoblotting using anti-Flag-HRP antibodies [21].

Flow cytometry assessment of ROS

Cellular levels of hydrogen peroxide and hydroxyl and peroxyl radicals (H_2O_2, OH^-, and ROO^-) were measured following staining with 5-(and-6)-carboxy-2',7'-dichlorodihydrofluorescein diacetate (DCFDA) (Invitrogen, Carlsbad, CA), while cellular levels of superoxide (O_2^-) were measured following staining with dihydroethidium (DHE) (Invitrogen, Carlsbad, CA) [35]. Stock solutions (20 mM) of the dyes were diluted with culture medium and added to cells to a final concentration of 5 µM DCFDA or 5 µM DHE. After incubating at 37°C in the dark for 30 min, cells were trypsinized, washed, and collected using PBS. The DCFDA and DHE signals were detected in the FL-1 (530 nm) and FL-2 channels (650 nm) respectively with a Becton, Dickinson FACS Calibur flow cytometer (BD, Franklin Lakes, NJ). A total of 10,000 events were measured per sample. Data were collected and analysed using CellQuest Pro and FlowJo software [21].

Glutathione levels

To assess the level of intracellular glutathione, cells were seeded into 96-well cell culture plates and allowed to grow for 24 hours under cell culture conditions. Cells were then treated with the BSO for 48 hours. Intracellular glutathione levels were measured using the bioluminescent Promega GSH-Glo™ glutathione assay kit according to the manufacturer's protocol (Promega, Madison, WI). Luminescence was detected using a MicroLumat Plus LB 96V bioluminometer (Berthold Technologies, Oak Ridge, TN).

Comet assessment of DNA damage

The comet assay was performed following the protocol provided with the Trevigen kit (Trevigen, Gaithersburg, MD). Briefly, cells were plated in agarose and spread over the sample area on slides. Alkaline electrophoresis using 21 V for 40 min was then performed. Nuclei were stained with SYBR gold (Invitrogen, Carlsbad, CA) and viewed by fluorescence microscopy. 100

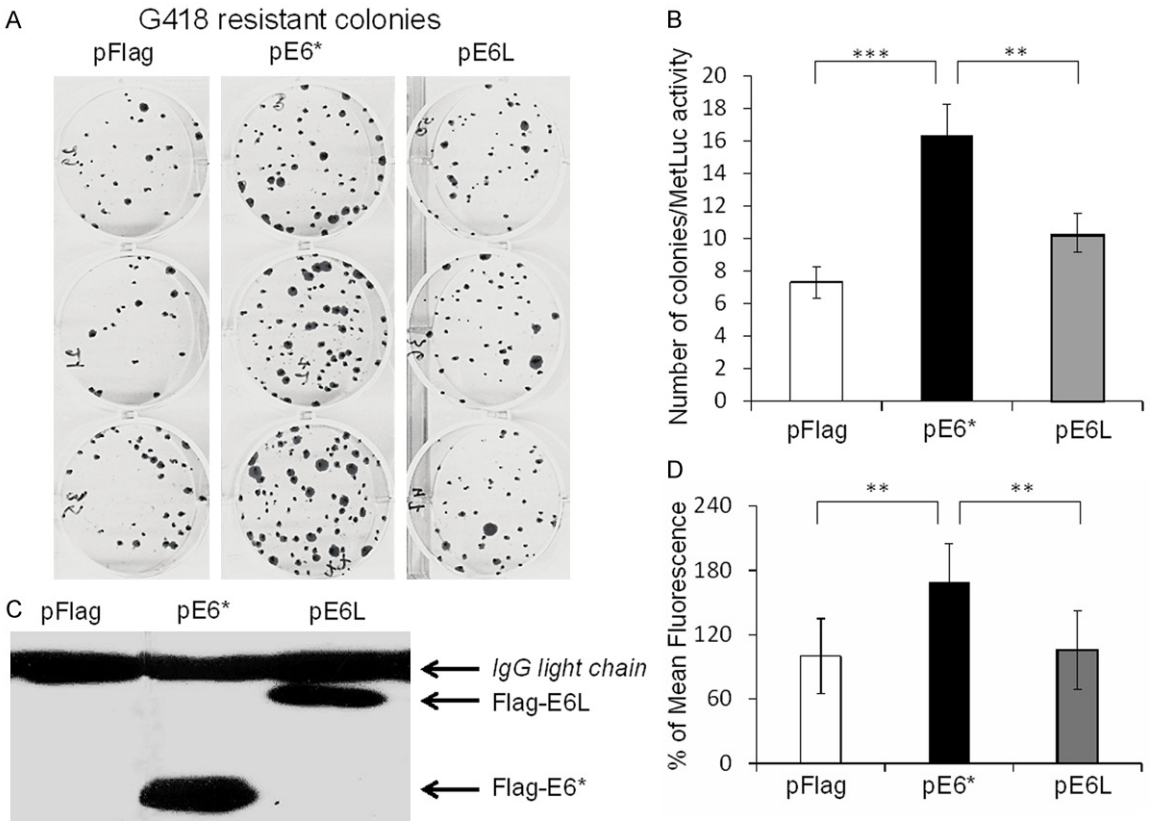

Figure 1. E6*, but not E6, increased the level of OS and the integration frequency of plasmid DNA into U2OS cells. A and B. 10^6 U2OS cells per well were co-transfected with plasmids encoding E6* (pE6*), E6 (pE6L) or vector (pFlag) together with the pMetLuc *puro* plasmid. To normalize for transfection efficiency, the media was collected 48 h post-transfection and the expression of secreted MetLuc (BD Clontech) was measured. Selection of cells resistant to *G418* (0.5 mg/ml) was performed for 3 weeks and the resulting colonies were stained with crystal violet. Colonies were counted after crystal violet staining (A) and normalized for transfection efficiency (B). C. Immunoprecipitation followed by immunoblot shows expression of Flag-E6* and Flag-E6L proteins after transient transfection. D. 10^5 cells per well of U2OS cells were transfected with plasmids encoding E6* (pE6*), E6 (pE6L) or vector (pFlag), and the level of cellular ROS was analysed 48 h post-transfection by fluorescence using a fluorescence plate reader following DCFDA staining. Triplicate measurements of mean fluorescence intensity of DCFDA were performed to generate the bar graphs of % mean fluorescence, setting the pFlag mean fluorescence at 100%.

DNA tails were photographed and analysed for each sample, and the length of each tail was measured from the center of the comet to the end of the tail using ImageJ software. Each cell was categorized as having tail lengths in one of four classes (0 to 50, undamaged; 50 to 100, minimum damage; 100 to 150, medium damage; >150, maximum damage) reflecting the severity of DNA damage. Tail lengths are known to increase proportionately with DNA damage [21].

APOT (amplification of papillomavirus oncogene transcripts)

The APOT assay was applied to detect and distinguish episomal- and integration-derived HPV transcripts. RNA from 5 × 10^6 cells was isolated using a Direct-zol RNA MiniPrep kit (Zymo research, Irvine, CA) as recommended by the supplier. Total RNA (1 mg) was reverse transcribed using a High Capacity cDNA Reverse Transcription Kit (Applied Biosystem by Life Technologies, Grand Island, NY), using an oligo $(dT)_{17}$-primer coupled to a linker sequence [$(dT)_{17}$-p3, 5'-GACTCGAGTCGACATCGATTTTTTT-TTTTTTTTTT-3'] and 1 µl of MultiScribe reverse transcriptase for 10 min at 25°C, then for 120 min at 37°C in a final volume of 20 µl.

APOT was performed as described previously by Klaes *et al.* [12]. Briefly, cDNAs were amplified by the first PCR round using HPV E7-specific oligonucleotides [p1 specific for HPV16 (5'-CGGACAGAGCCCATTACAAT-3') as forward primers and p3 (5'-GACTCGAGTCGACATCG-3') as

the reverse primer] in a 50 µl reaction mixture. The second PCR used forward primers p2 specific for HPV16 (5'-CTTTTTGTTGCAAGTGTGACTCTACG-3') and $(dT)_{17}$-p3 as the reverse primer in a total volume of 50 µl reaction mixture.

Amplification products were visualized by 1% agarose gel electrophoresis, and amplicons of sizes other than the episome-derived transcript (1050 bp) were subjected to further analysis [12]. PCR bands were extracted and cloned into pTOPO using the TOPO cloning reaction kit (Life Technologies, Grand Island, NY) and sequenced. The sequences obtained were compared to those within the HPV16 and human genomes to identify similar sequences, using National Center for Biotechnology Information (NCBI) Blast as well as UCSC Genome Bioinformatics Blat tools.

Quantitative reverse transcription PCR (qRT-PCR)

Reverse transcription was performed as described above (APOT). Quantitative real-time PCR was conducted to measure the levels of the E6 isoforms using primers designed as described previously by Hafner et al. [36], along with an Absolute QPCR SYBR Green Kit according to the manufacturer's protocol (Bio-Rad Laboratories, Hercules, CA). The observed E6 isoform concentrations were normalized using the level of phosphoglycerokinase (PGK) expression.

Results

E6, but not E6, increased the level of OS and the integration frequency of plasmid DNA into U2OS cells*

Previously, we demonstrated that overexpression of E6*, but not of the full-length E6 isoform, caused increased cellular levels of ROS and higher levels of oxidative DNA damage [21]. To investigate whether overexpression of E6* also increases the rate at which circular plasmid DNA integrates into the human genome, we performed a clonogenic assay. U2OS cells were transfected with plasmids encoding one of the HPV 16 E6 isoforms, E6* (pE6*) or the full-length E6 (pE6L), or with the empty vector (pFlag), along with a plasmid coding for G418 resistance. To normalize for transfection efficiency, the pMetLuc plasmid was co-transfected, and the expression of Metridia luciferase was monitored in the media. After G418 selection, the remaining colonies were stained with crystal violet and counted (**Figure 1A**). The normalized number of colonies is presented in **Figure 1B**. These data show that the number of colonies was higher when cells were transfected with pE6* than when transfected with the vector or the pE6 large plasmids (**Figure 1A**, **1B**). Immunoprecipitation followed by immunoblot analysis showed that E6* and E6 large were expressed in the corresponding cells (**Figure 1C**), and ROS levels following transient transfection with these plasmids, as estimated by fluorescence following DCFDA staining, were higher in cells transfected with E6* when compared to those transfected with pFlag or pE6L (**Figure 1D**). Overall, these results demonstrate that the short variant of the HR HPV E6 oncoprotein, E6*, but not the full-length variant (E6L), induces an increase in ROS and promotes the integration of plasmid DNA.

Increasing ROS results in increased integration frequency, while decreasing ROS results in decreased integration frequency

To examine the impact of OS on integration frequency, we increased or decreased the levels of ROS using agents known to affect cellular levels of these reactants. To carry out this set of experiments, we needed an agent that would induce chronic OS in our cells by modulating ROS levels without significantly affecting cell viability. We found that L-Buthionine-sulfoximine (BSO), which decreases the level of glutathione in cells through inhibition of gamma glutamyl cysteine synthetase (gamma GCS), the enzyme that catalyzes the first step of glutathione synthesis [37], was suitable for our needs. Application of BSO to U2OS cells at doses from 1.25 µM to 80 µM did not significantly affect cell viability, as assessed by crystal violet staining (**Figure 2A**), while treatment with 5 and 10 µM of BSO for 48 hours led to elevation of ROS levels, as assessed by flow cytometry following DCFDA staining (**Figure 2B**).

To determine whether chronic OS induced by BSO treatment increases the integration frequency of plasmid DNA in U2OS, we performed a clonogenic analysis of U2OS cells transfected with the pcDNA3 plasmid. After transfection, cells were plated onto a 6-well plate, and 3 wells were treated with 5 µM BSO for 5 days while the remaining 3 wells were used as con-

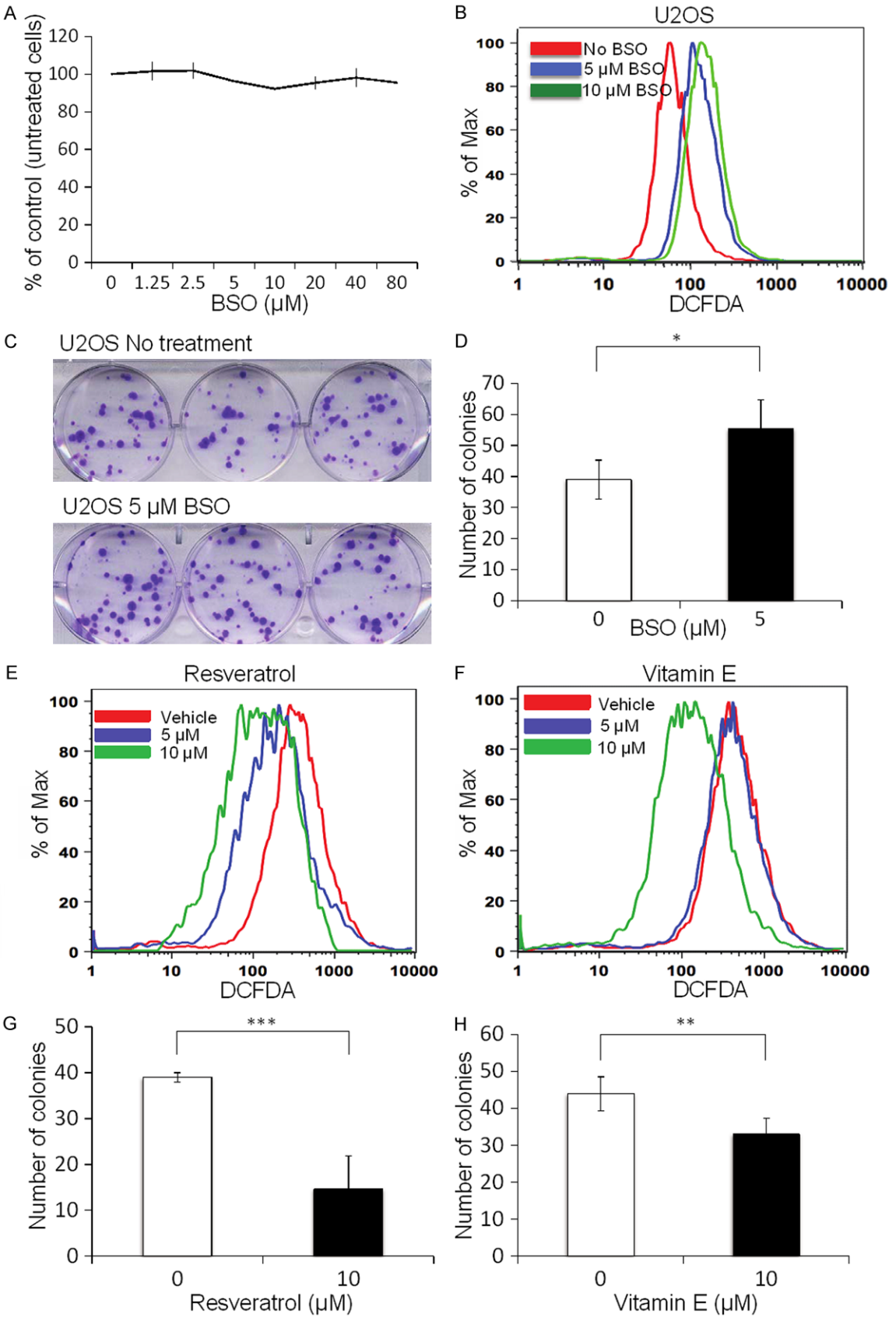
A
% of control (untreated cells)
120
100
80
60
40
20
0
0 1.25 2.5 5 10 20 40 80
BSO (μM)
B
U2OS
No BSO
5 μM BSO
10 μM BSO
% of Max
100
80
60
40
20
0
1 10 100 1000 10000
DCFDA
C
U2OS No treatment
U2OS 5 μM BSO
D
*
Number of colonies
70
60
50
40
30
20
10
0
0 BSO (μM) 5
E
Resveratrol
Vehicle
5 μM
10 μM
% of Max
100
80
60
40
20
0
1 10 100 1000 10000
DCFDA
F
Vitamin E
Vehicle
5 μM
10 μM
% of Max
100
80
60
40
20
0
1 10 100 1000 10000
DCFDA
G
***
Number of colonies
50
40
30
20
10
0
0 10
Resveratrol (μM)
H
**
Number of colonies
60
50
40
30
20
10
0
0 10
Vitamin E (μM)

Figure 2. Increasing ROS results in increased integration frequency, while decreasing ROS results in decreased integration frequency. A. U2OS cells (10^4 cells per well) were plated onto a 96-well plate, and cells were treated with BSO in triplicate at the indicated concentrations for 48 hours. Cell viability was estimated using the crystal violet assay. Cell viability without BSO treatment was set at 100%. B. The level of ROS in U2OS cells treated with the indicated concentrations of BSO for 48 h was estimated by flow cytometry following DCFDA staining. C. 1.5 × 10^5 cells per well of U2OS were transfected with the pcDNA3 plasmid, then plated onto a 6 well plate. After 24 hrs, 3 wells were treated with 5 μM of BSO for 5 days. Selection of cells resistant to *G418* (0.5 mg/ml) was performed for approximately 2 weeks, following which the colonies produced were stained with crystal violet. Colony numbers are presented in the bar graph (D). E, F. The level of ROS in U2OS cells treated with the indicated concentrations of resveratrol (E) and vitamin E (F) for 48 h was estimated by flow cytometry following DCFDA staining. G and H. 1.5 × 10^5 cells per well of U2OS were transfected with the pcDNA3 plasmid, then plated onto a 6 well plate. After 24 hrs, 3 wells were treated with 10 μM of resveratrol (G) or 10 μM of Vitamin E (H) for 48 h. Selection of cells resistant to *G418* (0.5 mg/ml) was performed for approximately 1 week, and the colonies produced were stained with crystal violet. Colony numbers are presented in the corresponding bar graphs (G) and (H). Error bars represent the standard deviation, *represents a 0.95 level of confidence, **represents a 0.99 level of confidence, and ***represents a 0.999 level of confidence.

trols. Following *G418* selection, the colonies were stained with crystal violet and counted (**Figure 2C**). The normalized number of colonies is presented in **Figure 2D**. These results demonstrate that chronic OS induced by BSO promotes the integration of plasmid DNA into U2OS cells.

To assess the effect of decreased ROS levels on integration frequency, cells were treated with the known antioxidants resveratrol [38] and vitamin E [39], and integration frequency was estimated using the clonogenic assay as described above. As expected, we found that ROS levels were significantly decreased after treatment with 5 μM and 10 μM resveratrol (**Figure 2E**) or with 10 μM Vitamin E (**Figure 2F**) for 48 hours as assessed by flow cytometry following DCFDA staining. After transfection with the pcDNA3 plasmid carrying the *G418*-resistant gene, cells were plated onto a 6-well plate, and 3 wells were treated with 10 μM resveratrol for 48 hours while the remaining 3 wells were left untreated. Following *G418* selection, the colonies were stained with crystal violet and counted (**Figure 2G**). A similar experiment was performed with U2OS cells treated with 10 μM Vitamin E (**Figure 2H**). These results clearly demonstrate that antioxidants that decreased ROS levels also caused a reduction in the rate at which circular plasmid DNA integrated into U2OS cells.

OS, induced by either overexpression of E6 or by glutathione depletion, increases DNA damage and the frequency of plasmid DNA integration into NOK cells*

To determine whether an increase of ROS in keratinocytes, the natural target cells for HPV infection, also results in an increased rate of circular DNA integration, we employed Normal Oral Keratinocytes (NOK), a cell line which was immortalized using hTERT (gift of Karl Münger) [31]. NOK cells stably expressing either E6* alone, E6, or the empty vector control were obtained as described previously following transduction of the retroviruses pLNCX-E6*, pLNCX-E6 or pLNCX, respectively [21]. We first employed qRT-PCR to compare the level of E6* expression in NOK-derived pE6*, pE6L and pLNCX cells with that seen in CaSki and SiHa cells, where E6* is expressed from integrated HPV16 [40], and with the level of E6* expressed in human cervical keratinocytes (HCK). The level of E6* expression in NOK pE6* cells was approximately 2 times higher than that observed in HCK and CaSki cells, suggesting that the level of E6* expression from the estimated 50-100 copies of the HPV genome in HCK cells is comparable to that seen from the integrated HPV in CaSki cells, and that expression of E6* from the E6*-expressing NOK cells is well within a two-fold range of levels seen physiologically (**Figure 3A**).

NOK cells expressing E6* are characterized by higher levels of ROS (**Figure 3B**) and DNA damage [21] than seen in NOK pLNCX or NOK E6L cells. To determine whether the plasmid integration rate was also higher in these cells, we transfected these pLNCX-E6*, pLNCX-E6 and pLNCX cells with the plasmid pMetLuc *puro*. To normalize for transfection efficiency, expression of secreted luciferase in the media was monitored. After *puromycin* selection, the number of colonies was counted after crystal violet staining (**Figure 3C**). This clonogenic assay revealed that NOK cells expressing E6* produced a higher number of colonies, as compared to NOK cells expressing either E6 or those transfected with the empty vector. These

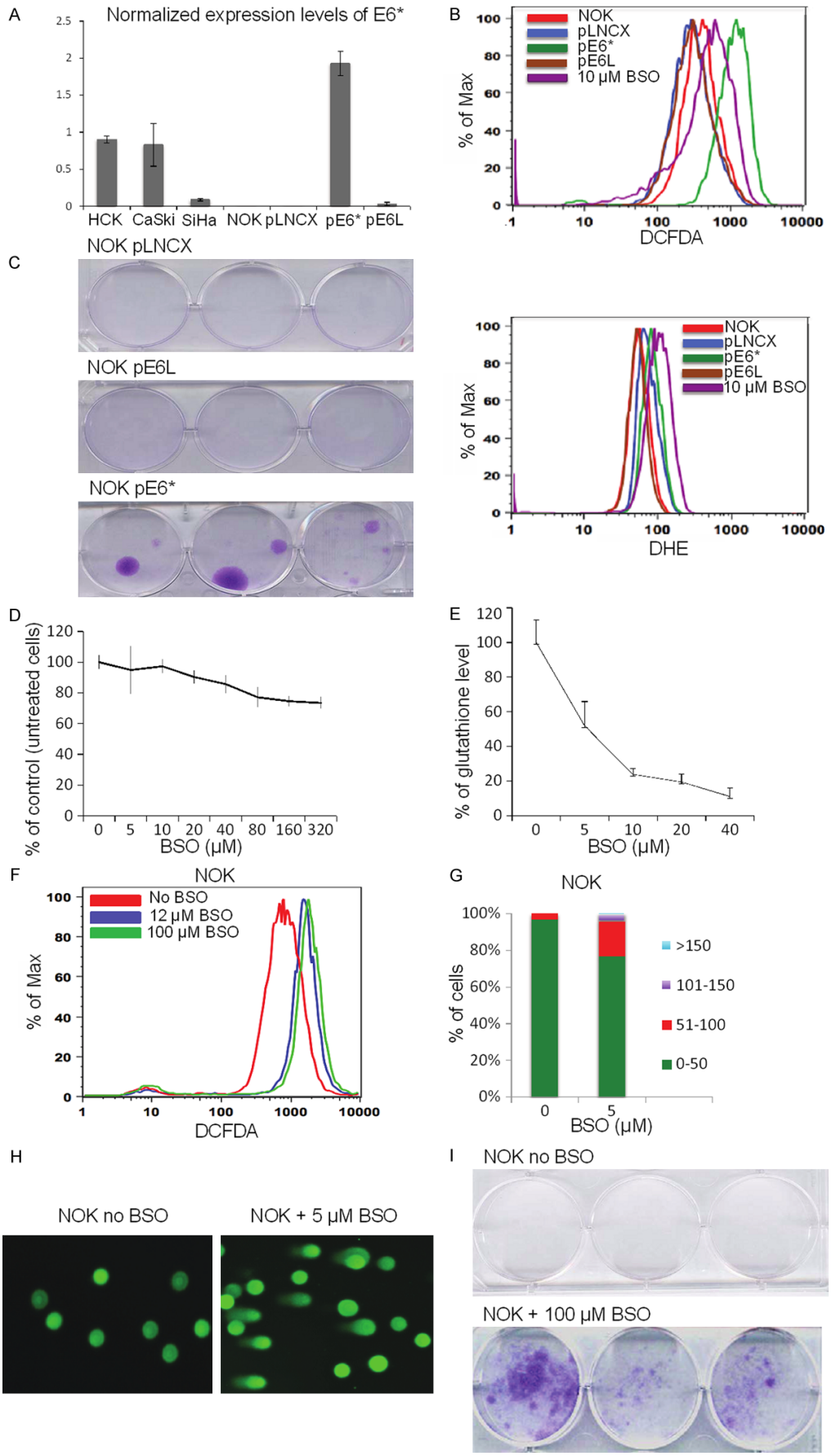
A
Normalized expression levels of E6*
HCK CaSki SiHa NOK pLNCX pE6* pE6L
B
NOK
pLNCX
pE6*
pE6L
10 μM BSO
% of Max
DCFDA
C
NOK pLNCX
NOK pE6L
NOK pE6*
DHE
D
% of control (untreated cells)
BSO (μM)
E
% of glutathione level
BSO (μM)
F
NOK
No BSO
12 μM BSO
100 μM BSO
% of Max
DCFDA
G
NOK
% of cells
>150
101-150
51-100
0-50
BSO (μM)
H
NOK no BSO
NOK + 5 μM BSO
I
NOK no BSO
NOK + 100 μM BSO

Figure 3. OS, induced by either overexpression of E6* or by glutathione depletion, increases DNA damage and the frequency of plasmid DNA integration into NOK cells. A. The expression levels of E6* transcripts in HCK, CaSki, SiHa, and NOK cell lines stably expressing either E6* alone (pE6*), E6 large (pE6L), or the empty vector (pLNCX) were analysed by qRT-PCR. E6* transcript expression levels were normalized by PGK gene expression. B. ROS levels in NOK-derived stable cell lines and NOK treated with 10 μM BSO were analysed by flow cytometry using DCFDA (upper panel) and DHE (lower panel) as described in Material and Methods. C. 10^6 cells per well of NOK-derived cell lines stably transduced with E6*, E6 large or the vector control were transfected with the pMetLuc *puro* plasmid. To normalize for transfection efficiency, media was collected 48 h post-transfection and the expression of secreted MetLuc was measured. Selection of cells resistant to *puromycin* (5 μg/ml) was performed for 3 weeks, and the colonies produced were stained with crystal violet. D. NOK cells (10^4 cells per well) were plated onto a 96-well plate, and cells were treated with BSO in triplicate at the indicated concentrations for 48 hours. Cell viability was estimated using the crystal violet assay. Cell viability without BSO treatment was set at 100%. E. 5×10^4 NOK cells were plated onto 24-well plates. After attachment, cells were treated with the indicated concentrations of BSO for 48 h. The resulting level of glutathione was measured using the Promega GSH-Glo™ glutathione assay kit according to the manufacturer's protocol. Measurements were performed in triplicate, and the glutathione level in untreated cells was set at 100%. F. The level of ROS in NOK cells treated with the indicated concentrations of BSO for 48 h was estimated by flow cytometry following DCFDA staining. G, H. NOK cells treated or untreated with 5 μM of BSO for 9 days, and the DNA damage was measured using the comet assay as described in Materials and Methods. G. 100 cells were counted per cell line and the percentage of cells with each tail length was calculated. H. Representative comet images of NOK cells untreated and treated with 5 μM BSO, visualized by microscopy following alkaline electrophoresis. I. 6×10^6 cells were transfected with the pMetLuc *puro* plasmid, then plated onto a 6 well plate. After 24 hrs, 3 wells were treated with 100 μM of BSO for 48 h. Selection of cells resistant to *puromycin* (5 μg/ml) was performed for 3 weeks and the resulting colonies were stained with crystal violet.

results demonstrate that overexpression of E6* results in an increase in ROS along with enhanced DNA integration into keratinocytes, similar to our observations in the U2OS model system.

To assess the impact of external, OS-inducing agents on DNA damage and integration in NOK cells, we again employed BSO. We found that BSO at concentrations ranging from 5 μM to 20 μM does not significantly affect cell viability, as assessed by crystal violet staining (**Figure 3D**). We also measured glutathione levels in these NOK cells before and after BSO treatment for 48 hours at several concentrations (5, 10, 20, and 40 μM) using the glutathione assay (Promega, Madison, WI). **Figure 3E** shows that BSO does, indeed, significantly reduce the level of glutathione in treated cells as compared to that seen in untreated cells. Treatment with BSO for 48 hours at concentrations of 12 and 100 μM in NOK cells increased ROS levels significantly (**Figure 3F**), as assessed by flow cytometry following DCFDA staining. Together, these results show that BSO is capable of inducing chronic cellular OS by decreasing levels of the antioxidant glutathione, without significantly affecting cell viability.

Next, we asked whether chronic OS induced by long-term BSO treatment would also increase DNA damage. NOK cells were treated with BSO for 9 days at a concentration of 5 μM, and DNA damage was estimated using the comet assay. The comet assay detects DNA strand breaks by measuring the distance DNA migrates out of cells (tail lengths), which corresponds to the severity of DNA damage [41]. The results of the comet assay (**Figure 3G**) demonstrate that the number of cells with longer tail lengths is increased in BSO-treated cells, as compared to an untreated control group. Representative cells with and without BSO treatment are shown in **Figure 3H**.

To determine whether chronic OS induced by BSO treatment also increases the integration frequency of plasmid DNA in keratinocytes, we performed a clonogenic analysis of NOK cells transfected with the pMetLuc *puro* plasmid. After transfection, cells were plated onto a 6-well plate, and 3 wells were treated with BSO for 48 hours while the remaining 3 were used as controls. Following *puromycin* selection of treated and untreated cells, the colonies were stained with crystal violet. No *puromycin* resistant clones were observed in wells without BSO treatment, while numerous stable clones were noted in wells treated with BSO (**Figure 3I**). These results clearly demonstrate that chronic OS induced by BSO promotes the integration of plasmid DNA.

The chronic OS that increased integration rates in NOK cells was induced by either overexpression of E6* (**Figure 3C**) or BSO treatment (**Figure 3I**). We compared the cellular levels of ROS resulting from E6 and E6* expression with

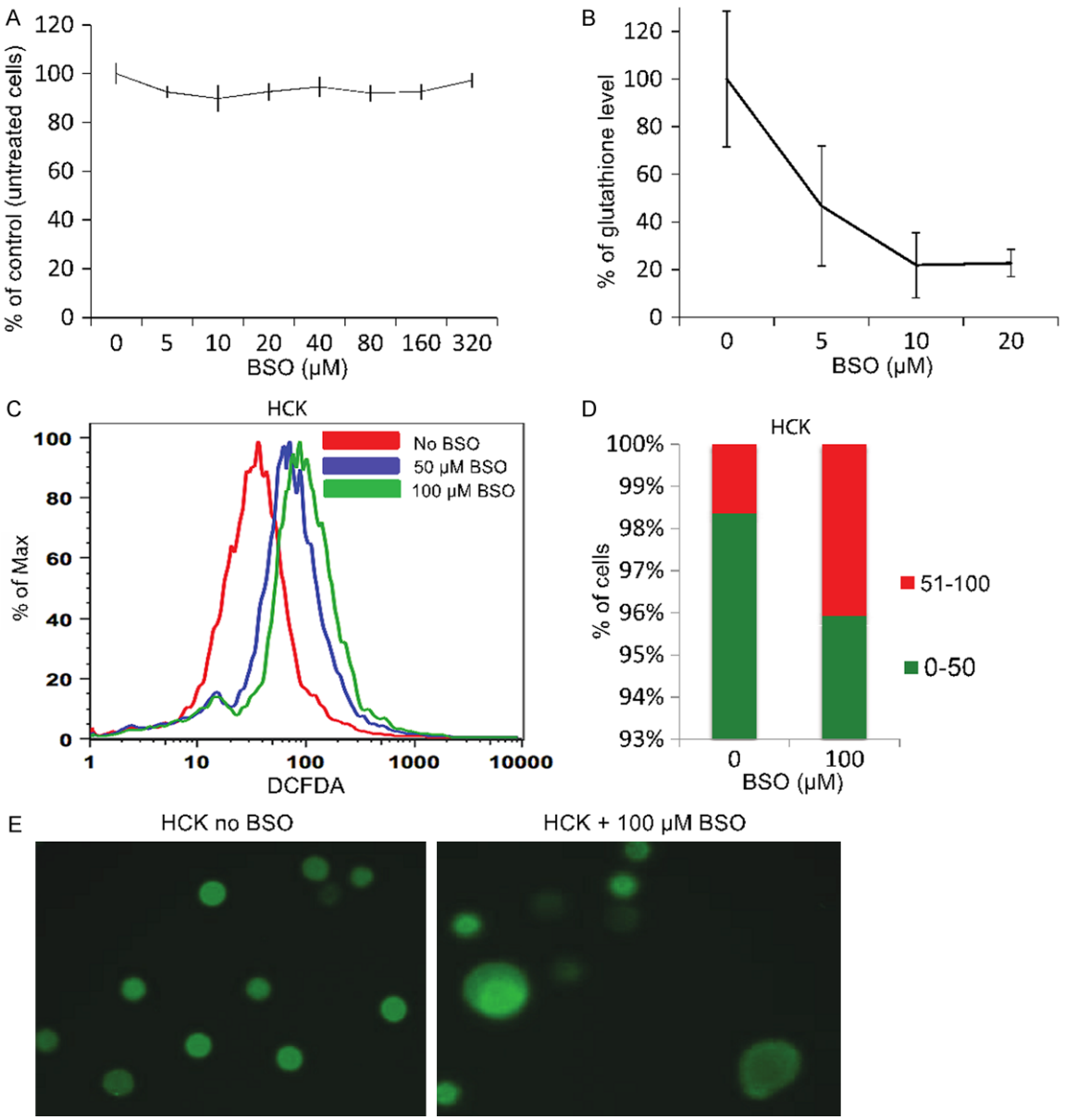

Figure 4. OS induced by glutathione depletion increases DNA damage in HCK cells containing episomal HPV16. A. 10^4 cells per well of HCK cells were plated onto a 96-well plate. Cells were treated with BSO in triplicate at the indicated concentrations for 48 hours. Cell viability was estimated by the crystal violet assay, with cell viability without BSO treatment set at 100%. B. 5 × 10^4 HCK cells were plated onto 24-well plates. After attachment, cells were treated with the indicated concentrations of BSO for 48 h. The level of glutathione was measured using the Promega GSH-Glo™ glutathione assay kit according to protocol. Measurements were performed in triplicate, and the glutathione level of untreated cells was set at 100%. C. The level of ROS in HCK cells untreated or treated with the indicated concentrations of BSO for 48 h was estimated by flow cytometry following DCFDA staining. D, E. HCK cells, were untreated or treated with 100 μM BSO for 8 days, then DNA damage was measured by the comet assay as described in Material and Methods. D. 100 cells were counted per cell line and the percentage of cells with each tail length was calculated. E. Representative comet images of HCK cells untreated or treated with 100 μM BSO, visualized by microscopy following alkaline electrophoresis.

those observed following treatment with 10 μM BSO. The results shown in **Figure 3B** demonstrate that exogenous application of the glutathione depleting agent BSO and expression of E6* in NOK cells lead to comparable levels of OS, suggesting that both environmental and viral factors may make significant contributions to the overall oxidative status.

OS induced by glutathione depletion increases DNA damage in HCK cells containing episomal HPV16

The results described above indicate that chronic OS exogenously induced by BSO increases the rate at which plasmid DNA integrates into NOK cells. To determine if OS stress is also able to promote the integration of episomal HPV into the genome of the host, we employed HPV-positive human cervical keratinocytes, HCK, in which the HPV genome is normally maintained in an episomal state. These cells were kindly provided by Aloysius J. Klingelhutz [32]. First, we determined the concentration range of BSO that was capable of increasing ROS levels without affecting cell viability in HCK cells. We found that BSO concentrations within the 5 μM to 320 μM range did not affect viability (**Figure 4A**), however, such BSO treatments were accompanied by decreases in glutathione levels (**Figure 4B**). Furthermore, concentrations of 50 and 100 μM BSO did significantly increase ROS levels in HCK cells after 48 hours of treatment (**Figure 4C**).

DNA damage in HCK cells following treatment with 100 μM BSO treatment for 8 days was evaluated using the Comet assay. The results presented in **Figure 4D** show that the relative number of cells with longer tail lengths was increased after BSO treatment, as compared to the untreated group. A representative comet assay is shown in **Figure 4E**. These results demonstrate that exogenous application of the glutathione depleting agent BSO can induce OS and increase DNA damage in HCK cells containing episomal HPV16.

Chronic OS increases the frequency of HPV16 genome integration in HCK cells containing episomal HPV16

To determine whether the DNA damage induced by chronic OS results in an increase in the frequency with which the HPV episome integrates into the genome, we employed the Amplification of Papillomavirus Oncogene Transcripts (APOT) assay. This assay detects fusion forms in integrated viral oncogene transcripts (**Figure 5A**) [12]. HCK cells were treated with BSO, and samples of treated cells were collected at days 10 and 17. Samples of untreated cells were collected, and all samples were kept frozen at -80°C prior to RNA isolation and performance of the assay. Results from the APOT assay are shown in **Figure 5B**. RNA isolated from CaSki and SiHa cells were used as controls for the integrated HPV genome, since both cell lines are known to contain integrated HPV16 [40].

An episomal HPV-derived transcript produces a 1050 bp product when assessed with a 5'-primer specific for the E7 region and a 3'-primer that binds to the poly-A tail region. If HPV is integrated, however, these primers will yield evidence of a fused transcript containing both HPV and human sequences. Hence, additional bands of different sizes will be observed [12]. The results of our APOT assay showed that PCR products from integration-derived transcripts in CaSki and SiHa cells were indeed of different lengths than the episomally-derived 1050 bp, showing that APOT detect fused transcripts [40] (**Figure 5B**, right two lanes). In HCK cells untreated with BSO, however, the most abundant band was found to be 1050 bp, confirming our expectation and previous reports that this cell line carries the episomal form of the virus [32] (**Figure 5B**, left-most lane). Treatment with BSO for either 10 or 17 days led to the appearance of 3 additional bands of lesser size (**Figure 5B**). It is worth noting that the intensity of these additional bands was stronger at day 17 than at day 10 (**Figure 5B**, lane 3 *vs* lane 2). These results suggest that integration-derived HPV transcripts do appear after long-term BSO treatment, consistent with our working model stating that chronic OS increases DNA damage and hence episomal integration. To determine whether these transcripts were indeed derived from integrated HPV, these additional bands of less than 1050 bp were cloned and sequenced. These additional bands contained chimeric sequences composed of HPV viral sequences together with cellular sequences. Direct sequencing showed that in each case, the breakpoints in HPV occurred in the region of the E7 gene, while the 3 human insertions occurred within 3 separate genes, CUX2, JRKL-AS1, and tRNaseZL-interacting RNA B1. Together, these data indicate that treatment with BSO, which increased the level of OS and DNA damage in these episome-harboring cells, led to 3 independent integration events in which episomal HPV was inserted into the host genome, and support a chain of events leading from the induction of oxidative stress, to DNA damage, and finally, to viral integration.

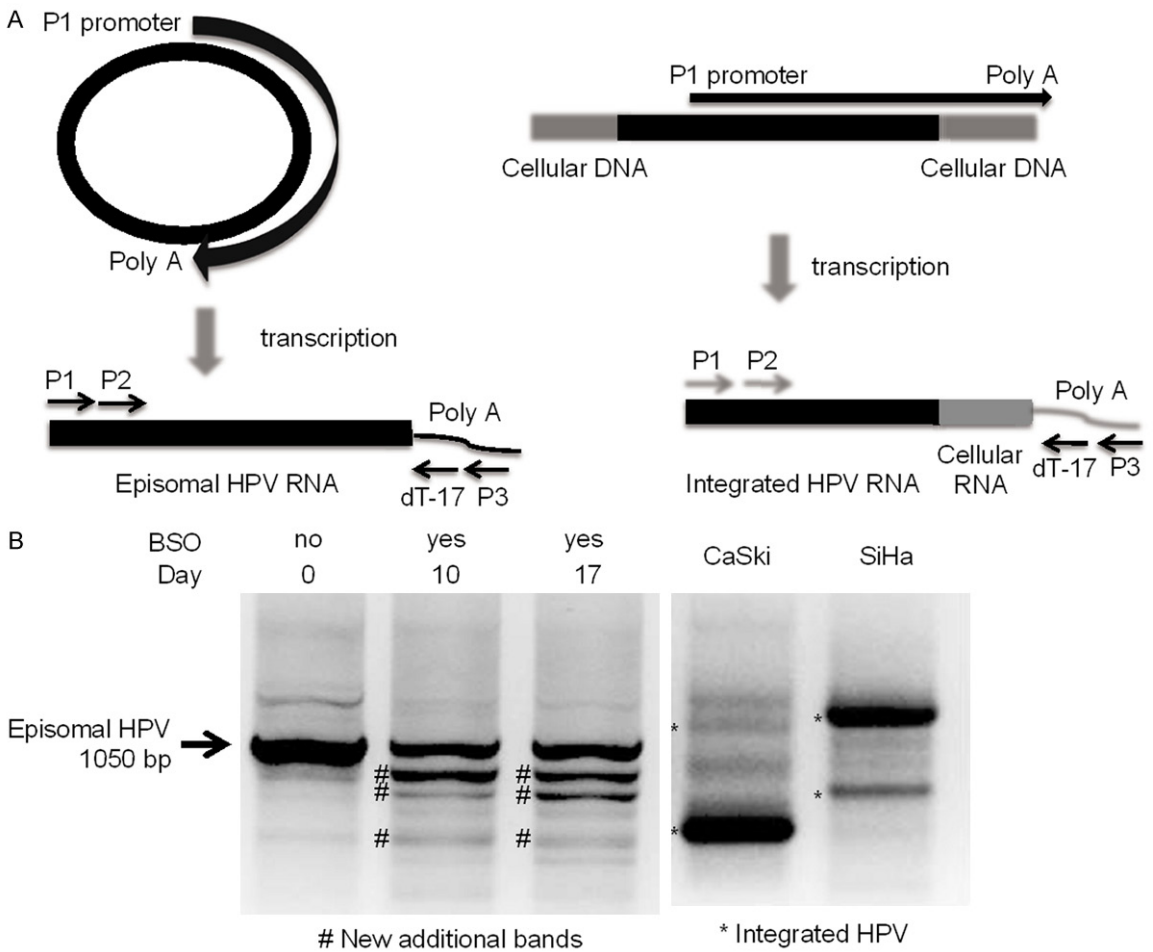

Figure 5. Chronic OS increases the frequency of HPV16 genome integration in HCK cells containing episomal HPV16. A. Scheme showing the Amplification of Papillomavirus Oncogene Transcripts (APOT) assay. Transcripts derived from either episomal (left) or integrated (right) HPV16 forms, as well as the location of primers used for the Reverse Transcriptase Reaction ($(dT)_{17}$-p3) for PCR (p1, p2, p3) are indicated (modified from *Ruediger Klaes, Stefan M. et al.* [12]). B. HCK were treated with 5 μm BSO for 10 and 17 days. RNA from these cells, together with that from untreated cells (days 0) was isolated, then used to perform the APOT assay as described in Material and Methods. RNAs isolated from CaSki and SiHa cells were used as controls for the integrated HPV genome. *labels the integrated HPV genome. #labels new additional bands corresponding to transcripts from integrated forms of HPV16. cDNA was synthetized using oligo-dT, and nested PCR was performed using primers specific for E7 and poly-A.

Discussion

In the work reported here, we tested the hypothesis that virus-mediated and/or environmental factors can induce chronic OS that contributes to DNA integration. Consistent with our working model, we demonstrated that indeed, chronic OS increases the integration rate of both plasmid DNA and the HR HPV genome.

Integration of plasmid DNA occurs in response to OS induction, as assessed by a clonogenic assay (**Figures 1A**, **1B**, **2C**, **2D**, **3C**, **3I**), as does HPV genome integration, as shown by APOT analysis (**Figure 5B**). These results are important because they demonstrate, for the first time, that the frequency of HPV integration can be manipulated by modulating levels of OS. It is generally accepted that high levels of ROS contribute to carcinogenesis by damaging DNA, RNA, proteins, and lipids, leading to cellular toxicity (reviewed in [24]). With respect to DNA, OS can induce DNA damage that results in apurinic/apyrimidinic (abasic) DNA sites, oxidized purines and pyrimidines, single-strand breaks (SSB) and double-strand breaks (DSB). These events further lead to chromosomal rearrangements and point mutations [18, 42]. With regards to DNA viruses, OS is particularly important in the context of HPV DNA integration, as ROS and reactive nitrogen species (RNS) have the potential to create the DSBs [30, 43]

that can in turn enable viral integration. Our ability to induce HPV integration provides us with a novel tool to experimentally study the initial steps of carcinogenesis using models that closely resemble an actual HPV infection.

Among the different mechanisms of viral carcinogenesis, integration of the viral genome into the host genome plays a critical role during the process of transformation by several oncogenic viruses including HBV, HPV, and Merkel cell polyomavirus (MCV). The connection between HBV integration and carcinogenesis is well accepted [44, 45], though the exact role of integration in Merkel cell carcinoma (MCC) carcinogenesis requires further study (reviewed in [18]). The connection between HPV integration and carcinogenesis is also widely accepted [8], and is largely based on analyses of patient tumor samples, as such cells present with integrated HPV at a very high frequency. However, this focus on fully transformed tissues limits the conclusions that can be drawn regarding factors that influence the integration events occurring prior to tumor development. Studies of tumor specimens indicate a lack of targeted disruption or functional alterations of critical cellular genes by the integrated viral sequences. Instead, most studies agree that integration occurs most frequently in common fragile sites (CFSs) [46] and in intronic sequences of human cellular genes [47] within (or adjacent to) oncogenes [46].

The three integration events we identified all involve a fusion between the E7 oncogene and a cellular sequence, with none of the three representing the type of integration event (between E2 and a cellular sequence) often observed in tumors. We therefore suggest that the integration of HPV genome into the host genome may be a much more frequent event than the initiation of transformation, and furthermore suggest that in most cases, this process is random and neutral in the context of cellular transformation. Consistent with our findings, a study from L. Turek's lab also shows that some identified HPV16 integration loci from head and neck cancer samples are involved in control of cell growth phenotype and oncogenes (16%), while other integration loci are neutral and varied, suggesting that not every integration of the virus will lead to carcinogenesis. The functional role of these viral integration events in the course of oncogenic progression remains to be defined [48].

Integration occurs rarely and represents a dead-end for the virus life cycle. However, accumulating evidence indicates that the machinery for HPV integration is likely provided by the HPV replication process [49], by way of activating the DNA Damage Response (DDR). Several DNA viruses, including HPV, have been shown to activate and utilize DNA repair mechanisms to enhance their own replication (review [50]). This is a reasonable link, since there is overlap between enzymes that mediate repair and those that participate in DNA replication. HPV viral DNA replication occurs in the nuclear foci, and expression of the E1 and E2 replication proteins is sufficient for the formation of replication foci that recruit components of the DDR [51-54]. HPVs enter the nucleus and initiate replication and transcription programs adjacent to nuclear domain 10 (ND10) bodies, which are associated with regions of DNA damage [55, 56]. Both E7 [57] and E1 [51] expression have been shown to activate the ATM-mediated DNA damage response. Although E6 inactivates the p53-mediated DNA damage repair pathway, p53-independent forms of DNA damage repair continue to function [57] and thereby support viral replication. Following DNA damage, recruitment of the repair apparatus to the linear viral episome and/or breaks in the host genome likely occurs. The recruitment of DNA damage repair complexes ensures the availability of ligases that can reconnect the recombined host and virus sequences, creating a microenvironment conducive to viral integration. In cases where the E1 and/or E2 regions are disrupted, these replication proteins are not expressed from integrated genomes but would be expressed from co-replicating, extrachromosomal HPV genomes, thereby inducing recruitment of DDR proteins to the integration loci, resulting in onion skin replication and promotion of genetic instability [58, 59]. Any modification that results in increased expression of the E6 and E7 oncoproteins is anticipated to further stimulate genetic instability and promote carcinogenesis [49]. The DDR can be induced by exogenous factors [60] and, as noted above, is likely involved in HPV integration.

In this current report, we showed that DNA damage induced through exogenous chronic OS increased integration of the HPV genome (**Figures 4A-E**, **5B**). DNA damage, and the resulting DDR, can also be induced by virus-derived factors, as the ability to damage DNA

has been reported for E2, E6, E6* and E7 [21, 61, 62]. In fact, our results demonstrated that E6* expression can induce DNA damage through increasing ROS levels and thereby promote foreign DNA integration (**Figures 1A**, **1B**, **2C**, **2D**, **3C**, **3I**). Factors other than OS can also promote integration of the viral genome. E6 and E7 expression have been shown to induce genome instability and contribute to an increased integration rate [20]; in addition, viral load and persistence have been demonstrated to promote integration [8, 63].

Importantly, we were able to successfully decrease the integration frequency by using antioxidants (resveratrol and vitamin E). These results (**Figure 2E-H**) are significant because they suggest that if chronic OS is indeed a factor promoting HR HPV integration, we have the potential to develop prophylactic and therapeutic strategies designed to prevent this initial step in carcinogenesis. Reduction of risk factors associated with chronic OS should be therefore considered as a prophylactic approach for the prevention of cervical cancer. Theoretically, therapeutic or dietary measures aimed at reducing oxidative stress could decrease oxidative stress in already-infected cells [64], and thereby diminish the risk of viral integration. In this report, we used the antioxidants vitamin E and resveratrol to reduce levels of cellular oxidative stress, which in turn reduced the integration of foreign DNA into U2OS cells. Our findings suggest that dietary antioxidants may be able to supplement the activity of endogenous antioxidants found in normal cells and fortify them against challenges posed by increased levels of ROS. In fact, studies have shown that several antioxidants are reduced in the circulation of cervical cancer patients [65]. A deficiency in antioxidant vitamins and/or other dietary components may, therefore, contribute to the increased prevalence of cervical cancer observed in women with a low socioeconomic status [65]. Possible benefits from dietary antioxidant consumption remain under discussion [64], and additional work is needed to test the effect of antioxidant therapies as a new approach for decreasing the probability of integration and thereby reducing cervical cancer incidence.

Overall, our results demonstrate that chronic OS can induce DNA damage and increase the frequency of HPV integration into the host genome, and in this way contribute to cervical carcinogenesis. Future strategies may focus on assessing cancer risk by screening for OS levels, then applying therapies directed toward OS, thereby decreasing the integration rate, and ultimately, carcinogenesis.

Acknowledgements

We thank Drs. Karl Münger and Aloysius Klingelhutz for kindly providing cells. We also thank our colleagues for helpful discussions and suggestions.

Disclosure of conflict of interest

None.

Address correspondence to: Dr. Penelope J Duerksen-Hughes, Department of Basic Science, Loma Linda University School of Medicine, Loma Linda, CA, 92354, USA. Tel: +1 909-558-4480; Fax: +1 909-558-4035; E-mail: pdhughes@llu.edu

References

[1] Parkin DM and Bray F. Chapter 2: The burden of HPV-related cancers. Vaccine 2006; 24 Suppl 3: S3/11-25.

[2] Bernard W, Stewart CP. Cancers of the female reproductive organs. World Cancer Report 2014 2014; 465-481.

[3] Ahn WS, Bae SM, Chung JE, Lee HK, Kim BK, Lee JM, Namkoong SE, Kim CK and Sin J. Evaluation of adenoassociated virus 2 and human papilloma virus 16 and 18 infection in cervical cancer biopsies. Gynecol Oncol 2003; 89: 105-111.

[4] Smith JS, Lindsay L, Hoots B, Keys J, Franceschi S, Winer R and Clifford GM. Human papillomavirus type distribution in invasive cervical cancer and high-grade cervical lesions: a meta-analysis update. Int J Cancer 2007; 121: 621-632.

[5] Lowy DR, Kirnbauer R and Schiller JT. Genital human papillomavirus infection. Proc Natl Acad Sci U S A 1994; 91: 2436-2440.

[6] Szalmas A and Konya J. Epigenetic alterations in cervical carcinogenesis. Semin Cancer Biol 2009; 19: 144-152.

[7] Baker CC, Phelps WC, Lindgren V, Braun MJ, Gonda MA and Howley PM. Structural and transcriptional analysis of human papillomavirus type 16 sequences in cervical carcinoma cell lines. J Virol 1987; 61: 962-971.

[8] Pett M and Coleman N. Integration of high-risk human papillomavirus: a key event in cervical carcinogenesis? J Pathol 2007; 212: 356-367.

[9] Rosty C, Sheffer M, Tsafrir D, Stransky N, Tsafrir I, Peter M, de Cremoux P, de La Roche-

fordiere A, Salmon R, Dorval T, Thiery JP, Couturier J, Radvanyi F, Domany E and Sastre-Garau X. Identification of a proliferation gene cluster associated with HPV E6/E7 expression level and viral DNA load in invasive cervical carcinoma. Oncogene 2005; 24: 7094-7104.

[10] Cullen AP, Reid R, Campion M and Lorincz AT. Analysis of the physical state of different human papillomavirus DNAs in intraepithelial and invasive cervical neoplasm. J Virol 1991; 65: 606-612.

[11] Peitsaro P, Johansson B and Syrjanen S. Integrated human papillomavirus type 16 is frequently found in cervical cancer precursors as demonstrated by a novel quantitative real-time PCR technique. J Clin Microbiol 2002; 40: 886-891.

[12] Klaes R, Woerner SM, Ridder R, Wentzensen N, Duerst M, Schneider A, Lotz B, Melsheimer P and von Knebel Doeberitz M. Detection of high-risk cervical intraepithelial neoplasia and cervical cancer by amplification of transcripts derived from integrated papillomavirus oncogenes. Cancer Res 1999; 59: 6132-6136.

[13] Dandri M, Burda MR, Burkle A, Zuckerman DM, Will H, Rogler CE, Greten H and Petersen J. Increase in de novo HBV DNA integrations in response to oxidative DNA damage or inhibition of poly(ADP-ribosyl)ation. Hepatology 2002; 35: 217-223.

[14] Petersen J, Dandri M, Burkle A, Zhang L and Rogler CE. Increase in the frequency of hepadnavirus DNA integrations by oxidative DNA damage and inhibition of DNA repair. J Virol 1997; 71: 5455-5463.

[15] Cougot D, Neuveut C and Buendia MA. HBV induced carcinogenesis. J Clin Virol 2005; 34 Suppl 1: S75-78.

[16] Hagen TM, Huang S, Curnutte J, Fowler P, Martinez V, Wehr CM, Ames BN and Chisari FV. Extensive oxidative DNA damage in hepatocytes of transgenic mice with chronic active hepatitis destined to develop hepatocellular carcinoma. Proc Natl Acad Sci U S A 1994; 91: 12808-12812.

[17] Shimoda R, Nagashima M, Sakamoto M, Yamaguchi N, Hirohashi S, Yokota J and Kasai H. Increased formation of oxidative DNA damage, 8-hydroxydeoxyguanosine, in human livers with chronic hepatitis. Cancer Res 1994; 54: 3171-3172.

[18] Chen Y, Williams V, Filippova M, Filippov V and Duerksen-Hughes P. Viral carcinogenesis: factors inducing DNA damage and virus integration. Cancers (Basel) 2014; 6: 2155-2186.

[19] Cerimele F, Battle T, Lynch R, Frank DA, Murad E, Cohen C, Macaron N, Sixbey J, Smith K, Watnick RS, Eliopoulos A, Shehata B and Arbiser JL. Reactive oxygen signaling and MAPK activation distinguish Epstein-Barr Virus (EBV)-positive versus EBV-negative Burkitt's lymphoma. Proc Natl Acad Sci U S A 2005; 102: 175-179.

[20] Kessis TD, Connolly DC, Hedrick L and Cho KR. Expression of HPV16 E6 or E7 increases integration of foreign DNA. Oncogene 1996; 13: 427-431.

[21] Williams VM, Filippova M, Filippov V, Payne KJ and Duerksen-Hughes P. Human papillomavirus type 16 e6* induces oxidative stress and DNA damage. J Virol 2014; 88: 6751-6761.

[22] Plummer M, Herrero R, Franceschi S, Meijer CJ, Snijders P, Bosch FX, de Sanjose S and Munoz N. Smoking and cervical cancer: pooled analysis of the IARC multi-centric case--control study. Cancer Causes Control 2003; 14: 805-814.

[23] Deacon JM, Evans CD, Yule R, Desai M, Binns W, Taylor C and Peto J. Sexual behaviour and smoking as determinants of cervical HPV infection and of CIN3 among those infected: a case-control study nested within the Manchester cohort. Br J Cancer 2000; 83: 1565-1572.

[24] Williams VM, Filippova M, Soto U and Duerksen-Hughes PJ. HPV-DNA integration and carcinogenesis: putative roles for inflammation and oxidative stress. Future Virol 2011; 6: 45-57.

[25] Finan RR, Musharrafieh U and Almawi WY. Detection of Chlamydia trachomatis and herpes simplex virus type 1 or 2 in cervical samples in human papilloma virus (HPV)-positive and HPV-negative women. Clin Microbiol Infect 2006; 12: 927-930.

[26] Hawes SE and Kiviat NB. Are genital infections and inflammation cofactors in the pathogenesis of invasive cervical cancer? J Natl Cancer Inst 2002; 94: 1592-1593.

[27] Castle PE and Giuliano AR. Chapter 4: Genital tract infections, cervical inflammation, and antioxidant nutrients--assessing their roles as human papillomavirus cofactors. J Natl Cancer Inst Monogr 2003; 29-34.

[28] Castle PE, Hillier SL, Rabe LK, Hildesheim A, Herrero R, Bratti MC, Sherman ME, Burk RD, Rodriguez AC, Alfaro M, Hutchinson ML, Morales J and Schiffman M. An association of cervical inflammation with high-grade cervical neoplasia in women infected with oncogenic human papillomavirus (HPV). Cancer Epidemiol Biomarkers Prev 2001; 10: 1021-1027.

[29] Wei L, Griego AM, Chu M and Ozbun MA. Tobacco exposure results in increased E6 and E7 oncogene expression, DNA damage and mutation rates in cells maintaining episomal human papillomavirus 16 genomes. Carcinogenesis 2014; 35: 2373-2381.

[30] Wei L, Gravitt PE, Song H, Maldonado AM and Ozbun MA. Nitric oxide induces early viral transcription coincident with increased DNA damage and mutation rates in human papillomavi-

rus-infected cells. Cancer Res 2009; 69: 4878-4884.
[31] Piboonniyom SO, Duensing S, Swilling NW, Hasskarl J, Hinds PW and Munger K. Abrogation of the retinoblastoma tumor suppressor checkpoint during keratinocyte immortalization is not sufficient for induction of centrosome-mediated genomic instability. Cancer Res 2003; 63: 476-483.
[32] Sprague DL, Phillips SL, Mitchell CJ, Berger KL, Lace M, Turek LP and Klingelhutz AJ. Telomerase activation in cervical keratinocytes containing stably replicating human papillomavirus type 16 episomes. Virology 2002; 301: 247-254.
[33] Wu YJ, Parker LM, Binder NE, Beckett MA, Sinard JH, Griffiths CT and Rheinwald JG. The mesothelial keratins: a new family of cytoskeletal proteins identified in cultured mesothelial cells and nonkeratinizing epithelia. Cell 1982; 31: 693-703.
[34] Filippova M, Song H, Connolly JL, Dermody TS and Duerksen-Hughes PJ. The human papillomavirus 16 E6 protein binds to tumor necrosis factor (TNF) R1 and protects cells from TNF-induced apoptosis. J Biol Chem 2002; 277: 21730-21739.
[35] Peshavariya HM, Dusting GJ and Selemidis S. Analysis of dihydroethidium fluorescence for the detection of intracellular and extracellular superoxide produced by NADPH oxidase. Free Radic Res 2007; 41: 699-712.
[36] Hafner N, Driesch C, Gajda M, Jansen L, Kirchmayr R, Runnebaum IB and Durst M. Integration of the HPV16 genome does not invariably result in high levels of viral oncogene transcripts. Oncogene 2008; 27: 1610-1617.
[37] Armstrong JS, Steinauer KK, Hornung B, Irish JM, Lecane P, Birrell GW, Peehl DM and Knox SJ. Role of glutathione depletion and reactive oxygen species generation in apoptotic signaling in a human B lymphoma cell line. Cell Death Differ 2002; 9: 252-263.
[38] Leonard SS, Xia C, Jiang BH, Stinefelt B, Klandorf H, Harris GK and Shi X. Resveratrol scavenges reactive oxygen species and effects radical-induced cellular responses. Biochem Biophys Res Commun 2003; 309: 1017-1026.
[39] Herrera E and Barbas C. Vitamin E: action, metabolism and perspectives. J Physiol Biochem 2001; 57: 43-56.
[40] Meissner JD. Nucleotide sequences and further characterization of human papillomavirus DNA present in the CaSki, SiHa and HeLa cervical carcinoma cell lines. J Gen Virol 1999; 80: 1725-1733.
[41] Collins AR. The comet assay for DNA damage and repair: principles, applications, and limitations. Mol Biotechnol 2004; 26: 249-261.
[42] Kryston TB, Georgiev AB, Pissis P and Georgakilas AG. Role of oxidative stress and DNA damage in human carcinogenesis. Mutat Res 2011; 711: 193-201.
[43] Ziech D, Franco R, Pappa A and Panayiotidis MI. Reactive oxygen species (ROS)--induced genetic and epigenetic alterations in human carcinogenesis. Mutat Res 2011; 711: 167-173.
[44] Brechot C, Pourcel C, Louise A, Rain B and Tiollais P. Presence of integrated hepatitis B virus DNA sequences in cellular DNA of human hepatocellular carcinoma. Nature 1980; 286: 533-535.
[45] Shafritz DA, Shouval D, Sherman HI, Hadziyannis SJ and Kew MC. Integration of hepatitis B virus DNA into the genome of liver cells in chronic liver disease and hepatocellular carcinoma. Studies in percutaneous liver biopsies and post-mortem tissue specimens. N Engl J Med 1981; 305: 1067-1073.
[46] Wentzensen N, Vinokurova S and von Knebel Doeberitz M. Systematic review of genomic integration sites of human papillomavirus genomes in epithelial dysplasia and invasive cancer of the female lower genital tract. Cancer Res 2004; 64: 3878-3884.
[47] Xu B, Chotewutmontri S, Wolf S, Klos U, Schmitz M, Durst M and Schwarz E. Multiplex Identification of Human Papillomavirus 16 DNA Integration Sites in Cervical Carcinomas. PLoS One 2013; 8: e66693.
[48] Lace MJ, Anson JR, Klussmann JP, Wang DH, Smith EM, Haugen TH and Turek LP. Human papillomavirus type 16 (HPV-16) genomes integrated in head and neck cancers and in HPV-16-immortalized human keratinocyte clones express chimeric virus-cell mRNAs similar to those found in cervical cancers. J Virol 2011; 85: 1645-1654.
[49] McKinney CC, Hussmann KL and McBride AA. The Role of the DNA Damage Response throughout the Papillomavirus Life Cycle. Viruses 2015; 7: 2450-2469.
[50] Lilley CE, Schwartz RA and Weitzman MD. Using or abusing: viruses and the cellular DNA damage response. Trends Microbiol 2007; 15: 119-126.
[51] Sakakibara N, Mitra R and McBride AA. The papillomavirus E1 helicase activates a cellular DNA damage response in viral replication foci. J Virol 2011; 85: 8981-8995.
[52] Fradet-Turcotte A, Bergeron-Labrecque F, Moody CA, Lehoux M, Laimins LA and Archambault J. Nuclear accumulation of the papillomavirus E1 helicase blocks S-phase progression and triggers an ATM-dependent DNA damage response. J Virol 2011; 85: 8996-9012.

[53] Reinson T, Toots M, Kadaja M, Pipitch R, Allik M, Ustav E and Ustav M. Engagement of the ATR-dependent DNA damage response at the human papillomavirus 18 replication centers during the initial amplification. J Virol 2013; 87: 951-964.
[54] Swindle CS, Zou N, Van Tine BA, Shaw GM, Engler JA and Chow LT. Human papillomavirus DNA replication compartments in a transient DNA replication system. J Virol 1999; 73: 1001-1009.
[55] Day PM, Baker CC, Lowy DR and Schiller JT. Establishment of papillomavirus infection is enhanced by promyelocytic leukemia protein (PML) expression. Proc Natl Acad Sci U S A 2004; 101: 14252-14257.
[56] Everett RD. Interactions between DNA viruses, ND10 and the DNA damage response. Cell Microbiol 2006; 8: 365-374.
[57] Moody CA and Laimins LA. Human papillomaviruses activate the ATM DNA damage pathway for viral genome amplification upon differentiation. PLoS Pathog 2009; 5: e1000605.
[58] Kadaja M, Sumerina A, Verst T, Ojarand M, Ustav E and Ustav M. Genomic instability of the host cell induced by the human papillomavirus replication machinery. EMBO J 2007; 26: 2180-2191.
[59] Kadaja M, Isok-Paas H, Laos T, Ustav E and Ustav M. Mechanism of genomic instability in cells infected with the high-risk human papillomaviruses. PLoS Pathog 2009; 5: e1000397.
[60] Giglia-Mari G, Zotter A and Vermeulen W. DNA damage response. Cold Spring Harb Perspect Biol 2011; 3: a000745.
[61] Duensing S and Munger K. The human papillomavirus type 16 E6 and E7 oncoproteins independently induce numerical and structural chromosome instability. Cancer Res 2002; 62: 7075-7082.
[62] Bermudez-Morales VH, Peralta-Zaragoza O, Guzman-Olea E, Garcia-Carranca A, Bahena-Roman M, Alcocer-Gonzalez JM and Madrid-Marina V. HPV 16 E2 protein induces apoptosis in human and murine HPV 16 transformed epithelial cells and has antitumoral effects in vivo. Tumour Biol 2009; 30: 61-72.
[63] Moberg M, Gustavsson I, Wilander E and Gyllensten U. High viral loads of human papillomavirus predict risk of invasive cervical carcinoma. Br J Cancer 2005; 92: 891-894.
[64] Garcia-Closas R, Castellsague X, Bosch X and Gonzalez CA. The role of diet and nutrition in cervical carcinogenesis: a review of recent evidence. Int J Cancer 2005; 117: 629-637.
[65] Manju V, Kalaivani Sailaja J and Nalini N. Circulating lipid peroxidation and antioxidant status in cervical cancer patients: a case-control study. Clin Biochem 2002; 35: 621-625.